IAI Journals.ASM.org

Natural History of Inhalation Melioidosis in Rhesus Macaques (*Macaca mulatta*) and African Green Monkeys (*Chlorocebus aethiops*)

John J. Yeager,[a] Paul Facemire,[b] Paul A. Dabisch,[a] Camenzind G. Robinson,[b] David Nyakiti,[a] Katie Beck,[c] Reese Baker,[a] and M. Louise M. Pitt[a]

Center for Aerobiological Sciences[a] and Pathology Division,[b] United States Army Medical Research Institute for Infectious Diseases, Fort Detrick, Maryland, USA, and Ke'aki Technologies LLC, Frederick, Maryland, USA[c]

***Burkholderia pseudomallei*, the causative agent of melioidosis, is recognized as a serious health threat due to its involvement in septic and pulmonary infections in areas of endemicity and is recognized by the Centers for Disease Control and Prevention as a category B biothreat agent. An animal model is desirable to evaluate the pathogenesis of melioidosis and medical countermeasures. A model system that represents human melioidosis infections is essential in this process. A group of 10 rhesus macaques (RMs) and 10 African green monkeys (AGMs) was exposed to aerosolized *B. pseudomallei* 1026b. The first clinical signs were fever developing 24 to 40 h postexposure followed by leukocytosis resulting from a high percentage of neutrophils. Dyspnea manifested 2 to 4 days postexposure. In the AGMs, an increase in interleukin 1β (IL-1β), IL-6, IL-8, gamma interferon (IFN-γ), and tumor necrosis factor alpha (TNF-α) was observed. In the RMs, IL-1β, IL-6, and TNF-α increased. All the RMs and AGMs had various degrees of bronchopneumonia, with inflammation consisting of numerous neutrophils and a moderate number of macrophages. Both the RMs and the AGMs appear to develop a melioidosis infection that closely resembles that seen in acute human melioidosis. However, for an evaluation of medical countermeasures, AGMs appear to be a more appropriate model.**

The bacterium *Burkholderia pseudomallei* is a Gram-negative bacillus typically found in tropical soil, standing water, rice paddies, and roots of plants (6, 22). In recent years, the traditional regions of endemicity of Southeastern Asia and Northern Australia have become more clearly defined. New areas of interest, which include India, China, areas of Africa, and South America, are arising (6, 11, 18). Melioidosis, which is the disease caused by *B. pseudomallei*, is becoming a more common occurrence in Thailand (24), Northern Australia (31), India (34), and Indonesia (6), typically causing infections in people performing activities that expose them to environments in which *B. pseudomallei* is prevalent (3). Especially at risk are persons with risk factors such as diabetes and excessive alcohol consumption (3, 8). Melioidosis is not recognized to occur as epidemics but can occur in outbreaks after abnormally intense monsoon rains and notably occurred as an outbreak after the 2004 tsunami in Indonesia (4, 6).

The three major exposure routes for melioidosis are inhalation, cutaneous inoculation, and ingestion (3, 7, 39). Inhalation is suspected of being the route that results in the most-acute infections (7, 17). Acute infections of melioidosis are characterized by fever, pneumonia, dyspnea, and sepsis (8, 26). The acute form of melioidosis has a rapid onset, with first symptoms developing within days to at most a few weeks after exposure (4, 26). Even with intensive intervention with intravenous antibiotics, the mortality rate of acute melioidosis can be 20 to 50% (2, 39). In chronic melioidosis, the clinical manifestations vary and can include chronic pneumonia, suppurative infections of skin, liver, kidney, or spleen, or a subclinical infection (8, 26).

Several animal models have been used to study melioidosis, including mice, hamsters, guinea pigs, and nonhuman primates (NHPs) (38). The most widely used melioidosis model system is the mouse. The murine model has been used to study many aspects of the host-pathogen interaction, which includes host immune system response, cytokine expression, tissue tropism, disease pathology, and disease progression (5, 13, 16, 19, 21, 23, 30, 35, 37). There are few reports of NHP models being used to study melioidosis, but one such study has suggested that rhesus macaques (RMs) challenged by subcutaneous injection with *B. pseudomallei* were relatively resistant (28). However, a second study in baboons suggests that NHPs are susceptible and develop an acute disease that is similar to that seen in humans (27). A recent study showed that the marmoset is susceptible to inhalational melioidosis and develops a lethal infection that closely resembles human infections (29).

To satisfy the FDA animal rule for evaluating medical countermeasures to melioidosis, a well-characterized animal model representative of the human disease is needed. Murine models have been shown to be effective; however, genetically, NHPs are more closely related to humans and an NHP model would be more desirable for evaluating medical countermeasures. We chose to evaluate the RM and the African green monkey (AGM) to determine if one or both are appropriate models to use for evaluation of medical countermeasures. Both the RM and the AGM have been used for other infectious disease models, yet conflicting data existed relating to the susceptibility of NHPs to melioidosis. Here we report the first steps in the development of the RM and the AGM as melioidosis disease models for medical countermeasure testing.

MATERIALS AND METHODS

Animal use. An equal mix of experimentally naive male and female AGMs (*Chlorocebus aethiops*, Saint Kitts) and RMs (*Macaca mulatta*, China)

Received 29 June 2012 Accepted 2 July 2012
Published ahead of print 9 July 2012
Editor: R. P. Morrison
Address correspondence to John J. Yeager, john.yeager3@us.army.mil.

doi:10.1128/IAI.00675-12

around 4 to 8 kg were exposed to aerosolized *B. pseudomallei* 1026b. All RMs and AGMs assigned to this study had physicals and were determined to be healthy. Preexposure complete blood counts (CBCs) and blood cultures were performed. All blood was negative for bacteria, and CBCs were within normal limits. Each NHP was implanted with a radio telemetry implant for measuring body temperature (TA10TA-D70; DSI, St. Paul, MN) or body temperature, blood pressure, and heart rate (TL11M2 D70-PCT; DSI, St. Paul, MN). A 4-min data segment was recorded hourly for the duration of the study (Dataquest ART; DSI, St. Paul, MN). All RMs and AGMs had single-lumen central venous catheters (CVCs) (Groshong 7F signal lumen; Bard Access System Inc., Salt Lake City, UT) surgically implanted to allow blood to be collected without anesthetizing the animals. All NHPs were monitored for disease symptoms daily. A humane endpoint was achieved for moribund animals by using behavioral and appearance assessments in addition to a drop in body temperature of greater than 2°C in 24 h or respirations of greater than 100 breaths per min (bpm). Research was conducted in compliance with the Animal Welfare Act and other federal statutes and regulations relating to animals and experiments involving animals and adheres to the principles stated in the Guide for the Care and Use of Laboratory Animals (28a). The facility where this research was conducted is fully accredited by the Association for Assessment and Accreditation of Laboratory Animal Care International.

Clinical observations. Clinical observations were performed a minimum of twice daily for the first 14 days postexposure and then a minimum of once daily thereafter. During observations, respiratory rates were recorded for each animal was and were used to evaluate dyspnea. Severe dyspnea was categorized as over 70 breaths per minute (bpm) (normal range, 26 to 38 bpm for RMs and 24 to 32 bpm for AGMs). Physical and behavior assessments were also performed to aid in determining moribund animals; this included observing food intake of enrichment foods (fruit and vegetables) and monkey biscuits to evaluate anorexia. Anorexia was defined as an observed decrease in food intake by at least half of the normal amount.

Bacterial strain. *B. pseudomallei* 1026b (obtained from D. Waag, USAMRIID) is a clinical isolate from Thailand which has been previously described (12).

Bacterial preparation. *B. pseudomallei* 1026b at a concentration of about 5.0×10^9 was stored in 500-μl aliquots in a −70°C freezer. The day before use, the vials were thawed and the contents were placed into 200 ml of glycerol tryptone broth (GTB; 10 g/liter tryptone [DB, Franklin Lakes, NJ], 5 g/liter NaCl, and 4% glycerol) in a 2-liter flask and incubated on a shaker platform at 37°C for 22 to 26 h to allow the bacteria to enter stationary phase. Immediately before the aerosol exposure, the freshly grown stock of *B. pseudomallei* was diluted to the appropriate concentration in GTB.

Aerosol exposure. The NHPs were exposed to a small-particle aerosol of *B. pseudomallei* 1026b in a well-characterized, dynamic, head-only exposure chamber that was controlled by an automated bioaerosol exposure system (10, 15). Before aerosol exposure, each NHP was anesthetized by intramuscular injection with 0.1 mg/kg of body weight of a ketamine-acepromazine mixture for AGMs and 3 mg/kg of tiletamine-zolazepam (Telazol) for RMs. Each animal was placed into a head-out plethysmography chamber and the minute volume (MV) was measured for 3 min (BioSystem XA; Buxco, Wilmington, NC). The average MV was used to adjust the exposure time to achieve the same target dose for all animals. The aerosol was generated using a 3-Jet Collison nebulizer (BGI Inc., Waltham, MA), and particle size was measured using an aerodynamic particle sizer with a 100:1 air dilution (APS Model 3321; TSI, Shoreview, MN). Samples of the aerosol atmosphere were collected using 25-mm gelatin filters (SKC, Eighty Four, PA) and all-glass impingers (Model 7541; Ace Glass Inc., Vineland, NJ) with a collection medium of GTB. Samples were titrated to determine the average concentration of the aerosol atmosphere. Individual aerosol exposure doses were calculated as the product of the average aerosol concentration within the chamber and the total volume of air breathed by the subject (product of MV and exposure duration).

Blood collection. Blood was collected by the CVC into EDTA (~1 ml) or serum separation tubes (~1 ml). Blood was collected for baseline values, once daily for the first 7 days postexposure, and then once weekly until the end of the study. For 5 RMs and 5 AGMs, an additional ~0.5 ml of blood was collected at 8-h intervals from 24 to 72 h postexposure into EDTA only.

Hematology. Samples were collected in EDTA-treated tubes. CBCs were performed using a CellDyne 3700 (Abbott Diagnostics, Abbott Park, IL). Leukopenia or leukocytosis was determined using reference ranges for RMs and AGMs. The normal reference range was 1.8×10^3 to 12.7×10^3 cells/μl for the RM and 2.1×10^3 to 8.9×10^3 cells/μl for the AGM. Similarly, neutrophilia or neutropenia was determined using the reference ranges of 0.5×10^3 to 9.2×10^3 cells/μl for the RM and 0.5×10^3 to 4.3×10^3 cells/μl for the AGM.

Bacterial dissemination. Two 100-μl samples of whole blood were plated at days 1 to 7, 14, 21, 28, 35, and 42 postexposure on glycerol tryptone agar (GTA; prepared the same way as GTB with 15 g/liter agar [BD, Franklin Lakes, NJ]) to detect bacteremia. Each plate was incubated at 37°C for 72 h. Tissue samples from the lung, liver, spleen, pancreas, and gonads were sterilely collected at necropsy and cultured for bacteria. Each tissue sample of approximately 0.25 to 1.0 g was homogenized in 2 ml GTB, and two 100-μl samples were plated on GTA to evaluate positive or negative growth.

Cytokines and chemokines. Serum was collected in serum separation tubes, and samples were distributed to aliquots and frozen at −80°C until analysis was performed using a human proinflammatory 9-plex kit on a Sector Imager 2400 (MesoScale Diagnostics, Gaithersburg, MD).

Gross pathology and histopathology. A full necropsy was performed on all animals by a board-certified veterinary pathologist. Tissues were collected and immediately immersed in 10% neutral buffered formalin (NBF). Tongue, tonsil, salivary gland, nares, lip, larynx, trachea, esophagus, thyroid gland, parathyroid gland, lung, heart, aorta, thymus, liver, gallbladder, spleen, kidneys, urinary bladder, reproductive organs, pituitary gland, adrenal gland, mandibular lymph node, mediastinal lymph node, tracheobronchial lymph node, mesenteric lymph node, axillary lymph node, inguinal lymph node, stomach, pylorus, duodenum, pancreas, jejunum, ileum, ileocecal junction, colon, haired skin, mammary gland, skeletal muscle, sciatic nerve, brachial plexus, brain, and eyes were submitted from all NHPs for histopathology. The nasal cavity was submitted from some but not all NHPs. Tissues were fixed for a minimum of 21 days in NBF. Tissue sections were trimmed at 5- to 6-μm thickness and stained with hematoxylin and eosin.

Immunohistopathology. Unstained tissue sections were deparaffinized, rehydrated, subjected to a methanol hydrogen peroxide block for 30 min, and then rinsed in phosphate-buffered saline (PBS). A serum-free protein block plus 5% normal goat serum was applied for 30 min. A monoclonal mouse antibody (3B3-5) to lipopolysaccharide (LPS) of *B. pseudomallei* (D. Waag, USAMRIID; prepared as previously described for *B. mallei* [36]) was diluted 1:1,200 and incubated at room temperature for 60 min. A polymer-labeled horseradish peroxidase anti-rabbit secondary antibody (EnVision Plus System; Dako Corp., Carpinteria, CA) was applied for 30 min at room temperature. All sections were exposed to 3,3′-diaminobenzidine (DAB) for about 5 min, rinsed, counterstained with hematoxylin, dehydrated, and coverslipped with Permount. To evaluate cross-reactivity and background staining, control samples of tissue infected with *Yersinia pestis*, *Francisella tularensis*, *Bacillus anthracis*, or poxvirus and normal tissue (uninfected) were tested, and no 3B3-5 immunoreactivity was observed. Tissue infected with *B. mallei* had minimal immunoreactivity. Additionally, no background staining was observed when an isotype control mouse IgG antibody was used to evaluate nonspecific binding of 3B3-5. Six NHPs (three RMs and three AGMs) were selected by three different time points comprised of two acute cases (3 to

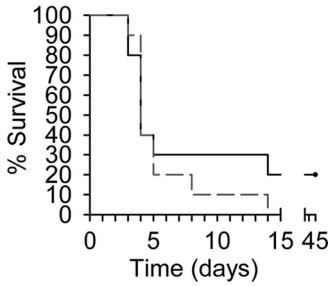

FIG 1 Survival curves for RMs and AGMs. Ten RMs (solid line) and AGMs (dashed line) were exposed to 3,796 ± 1,883 CFU and 3,239 ± 803 CFU, respectively. The median time to death for both the RMs and the AGMs was 4 days (95% CI, 3 to 5 days). There was no significant difference in survival times between RMs and AGMs ($P = 0.43$) or between males and females ($P = 0.72$).

4 days), two subacute to chronic cases (14 days), and two study survivors (45 days).

Ultrastructural pathology. Samples of lung, spleen, and tracheobronchial lymph node were collected at necropsy, trimmed to ~1 mm^3, and immersed in a mixed aldehyde fixative in a 0.1 M phosphate buffer. Samples were fixed for a minimum of 24 h, buffer washed, and immersed in 1% osmium tetroxide in the same buffer for 1 h. Before further contrasting, samples were buffer washed, rinsed in 50% ethanol, contrasted in ethanolic uranyl acetate, and dehydrated in an ascending series of ethanol. Propylene oxide (PO) was utilized as a transition solvent, and samples were infiltrated in 100% PO, a 50:50 mix of PO and EMbed-812 epoxy resin, or pure EMbed-812. Samples in pure resin were polymerized by incubation at 60°C for no less than 24 h. Embedded samples were sectioned at ~70 nm on a Leica ultramicrotome, mounted on copper mesh grids, and contrasted with uranyl and lead salts. Sections were examined on a JEOL 1011 transmission electron microscope at 80 kV. Digital images were acquired using a Hamamatsu ORCA-HR digital camera controlled by AMT image acquisition software. Micrographs were cropped and globally adjusted for contrast in Adobe Photoshop.

Statistical analysis. Statistical analysis was performed using SigmaPlot 11 (Systat Software Inc., San Jose, CA). Kaplan-Meier log-rank survival analysis was used to construct survival curves, calculate the median survival time and 95% confidence intervals (CI), and compare significance between groups. Analyses of complete blood counts and $\log_{10}$-transformed cytokine and chemokine data were performed using a two-way repeated-measures analysis of variance (ANOVA). Correlations between increased survival time and increased neutrophil, lymphocyte, and monocyte levels and between survival time and cytokine levels were done using the Spearman rank order test.

RESULTS

Exposure to aerosolized *B. pseudomallei*. For future replication of these inhalation models, it is critical to document the aerosol atmosphere that was presented to the animals. To characterize the aerosol atmosphere, the particle size, temperature, and humidity were measured for each exposure. The aerosol had a mass median aerodynamic diameter of 1.86 ± 0.05 μm (geometric standard deviation, 1.88 ± 0.02) and was at a temperature of 24.9°C ± 0.5°C and relative humidity of 46.7% ± 4.1%.

A total of 20 NHPs, 10 RMs and 10 AGMs, were exposed to aerosolized *B. pseudomallei* 1026b. The 10 RMs were exposed to 3,796 ± 1,883 CFU, and the 10 AGMs were exposed to 3,239 ± 803 CFU. A total of 8/10 RMs and 10/10 AGMs became moribund (Fig. 1). Two RMs survived the 45-day observation period, one with minimal clinical signs of infection after 14 days (1,763 CFU) and a second surviving with symptoms of chronic pneumonia (6,239 CFU). There was no significant difference in survival time between the RMs and AGMs ($P = 0.43$) or between males and females ($P = 0.72$).

Clinical signs of acute inhalation melioidosis. Melioidosis commonly presents with fever. To monitor the progression of the febrile response, body temperature was monitored hourly by radio telemetry. The febrile response was found to be one of the primary indications of disease (Table 1). Fever was characterized by abrupt onset and loss of diurnal rhythm in both RMs and AGMs. A sustained fever of more than 1.5°C above individual baseline temperatures (about 38.5°C) developed in 10/10 RMs at 32.4 ± 6.0 h postexposure and 10/10 AGMs at 34.1 ± 3.7 h postexposure (Fig. 2A and B). The two RMs that survived 45 days postexposure had a fever early in their infection that resembled that of moribund animals, but the fever gradually subsided for one RM (Fig. 2C). The second RM maintained an elevated diurnal temperature for the duration of the study.

To track the progression of symptoms of acute melioidosis, daily clinical evaluations were performed. One of the most pronounced clinical signs of acute melioidosis was dyspnea. Dyspnea was categorized as severe in 8/10 RMs and 9/10 AGMs (Table 1), which includes one RM that survived for 45 days postexposure. One RM and one AGM had mild dyspnea, and the other RM that survived for 45 days postexposure had mild dyspnea that subsided by day 14. A cough was observed in 3/10 RMs (Table 1). Additionally, mild anorexia was noted to occur 24 h before the animals became moribund in both the RMs and AGMs.

Change in blood parameters after exposure to *B. pseudomallei*. Melioidosis is known to be accompanied by large increases in neutrophils postexposure. To evaluate the neutrophil response, in addition to other blood parameters postexposure, blood was collected at various times pre- and postexposure. Leukocytosis resulting from a high percentage of neutrophils was commonly observed (Table 1 and Fig. 3A and B). The observed trend of leukocytes was an increase until 2 days postexposure and then a gradual decrease in animals that survived the longest and a more rapid decrease in animals that became moribund within 5 days postexposure (Fig. 3A and B). In 3/10 RMs and 2/10 AGMs, leukopenia was observed within 24 h of becoming moribund (Table 1). The percentage of neutrophils increased starting 24 h postex-

TABLE 1 Clinical manifestations of inhalation melioidosis

Manifestation	Prevalence (no. with manifestation/ total no.)		Range of onset (no. of days postexposure)
	RMs	AGMs	
Fever[a]	10/10	10/10	1–2
Leukocytosis[b]	10/10	10/10	1–2
Neutrophilia[c]	10/10	10/10	1–2
Bacteremia	9/10	7/10	1–4
Severe dyspnea[d]	8/10	9/10	2–4
Leukopenia[e]	3/10	2/10	3–5
Cough	3/10	0/10	3–7
Anorexia[f]	10/10	10/10	3–7

[a] Greater than 1.5°C above baseline (around 38.5°C).
[b] Greater than 12.7×10^3 cells/μl (RMs) and 8.9×10^3 cells/μl (AGMs).
[c] Greater than 9.2×10^3 cells/μl (RMs) and 4.3×10^3 cells/μl (AGMs).
[d] Greater than 70 bpm.
[e] Less than 1.8×10^3 cells/μl (RMs) and 2.1×10^3 cells/μl (AGMs).
[f] Less than half of normal food intake.

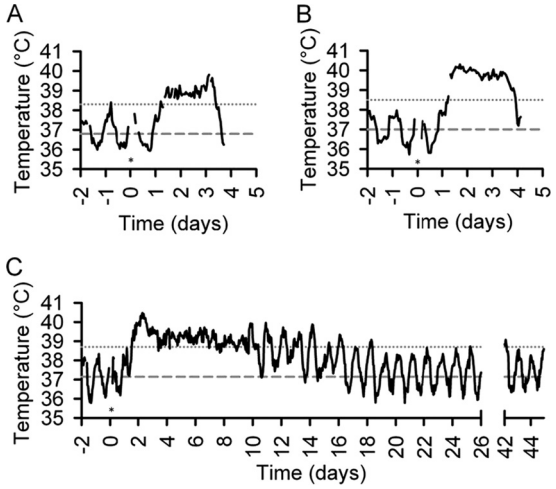

FIG 2 Representative temperature profiles of RMs and AGMs with melioidosis. Acute melioidosis was characterized by the abrupt increase in temperature and loss of the normal diurnal rhythm. By day 1 (24 to 40 h) postexposure, the temperature had reached the fever threshold (dotted line, 1.5°C above baseline); by 2 days postexposure, all RMs and AGMs exposed to *B. pseudomallei* developed a fever of 1.5°C to 2.5°C above the mean baseline temperature (dashed line). Representative body temperature profiles of an RM that was exposed to 1,824 CFU (A) and an AGM exposed to 2,186 CFU (B) show the characteristic rapid increase and the loss of normal diurnal rhythm. Both of those temperature profiles (A and B) are representative of all RMs and AGMs within the first 3 days postexposure. (C) One RM that was exposed to 1,763 CFU survived for 45 days postexposure, developing a sustained fever for about 10 days which then, over the next week, gradually subsided, returning to normal around 18 days postexposure. *, aerosol exposure.

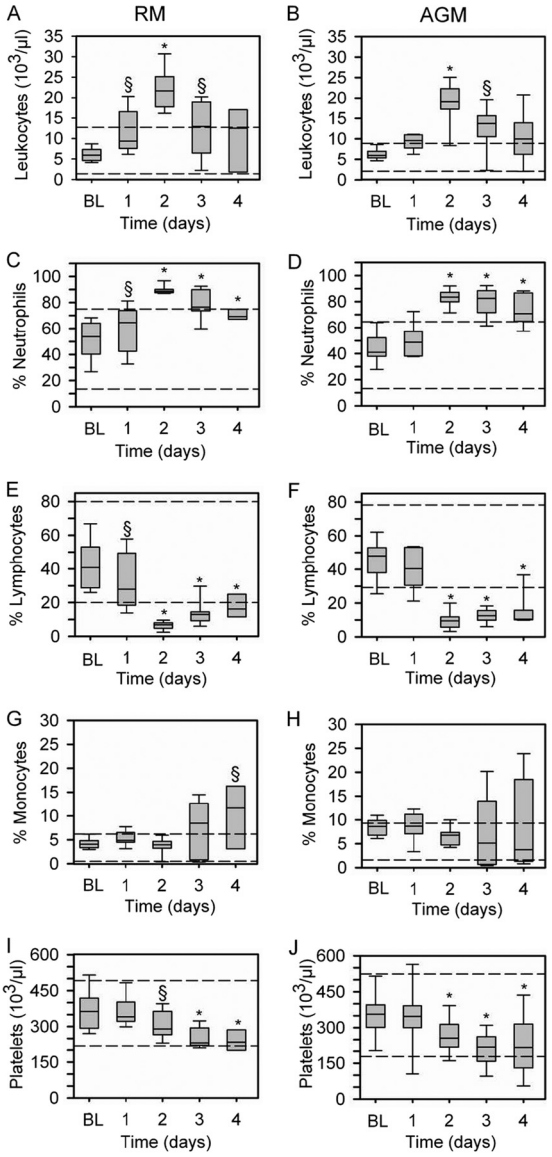

FIG 3 Hematology of RMs and AGMs after exposure to *B. pseudomallei*. A significant increase in leukocytes was observed 2 days postexposure in both the RMs (A) and AGMs (B), with a decreasing trend 3 and 4 days postexposure. An increase in the percentage of neutrophils was observed (RMs, panel C; AGMs, panel D), with a corresponding decrease in lymphocytes at day 2 through day 4 postexposure (RMs, panel E; AGMs, panel F). (G) In the RMs, a general increase in the percentage of monocytes was observed. (H) In the AGMs, the percentages of monocytes were highly variable, with most decreasing by day four and other increasing. Platelet levels decreased in the RMs (I) and AGMs (J) starting 2 days postexposure and continuing through 4 days postexposure. There was no significant difference between RMs and AGMs. Horizontal dashed lines represent the normal expected range, bars represent the 25th and 75th percentiles (the solid line is the median), and error bars represent the 5th and 95th percentiles. Baseline (BL), day 1, day 2, and day 3, $n = 10$; day 4, $n = 8$ and $n = 9$ for RMs and AGMs, respectively. §, $P < 0.05$; *, $P < 0.001$.

posure (Fig. 3C and D), corresponding with a decrease in the percentage of lymphocytes in all RMs and AGMs (Fig. 3E and F). The percentage of monocytes was variable; however, an increase was noted 4 days postexposure in the RMs (Fig. 3G) and AGMs (Fig. 3H). It was observed that the two surviving RMs had elevated monocyte levels. To determine if monocyte levels correlate to increased survival, pooled monocyte, lymphocyte, and neutrophil levels of RMs and AGMs for day 3 postexposure were evaluated using the Spearman rank order test. It was found that survival time increased when levels of monocytes ($P = 0.005$) and lymphocytes ($P = 0.002$) increased but not when levels of neutrophils increased ($P = 0.12$). A significant decrease in platelets was noted in both the RMs (Fig. 3I) and the AGMs (Fig. 3J). A decrease in red blood cells (RBC) was significant in the AGMs ($P < 0.001$); this was not noted in the RMs. Additionally, hematocrit ($P < 0.001$) and hemoglobin ($P < 0.001$) levels decreased in AGMs, but the changes were again not significant in the RMs. There was no significant difference between RMs and AGMs for leukocytes, neutrophils, lymphocytes, monocytes, or platelets. There was a significant difference between RMs and AGMs in levels of RBC ($P = 0.001$), hematocrit ($P < 0.001$), and hemoglobin ($P < 0.05$).

Septicemia in melioidosis results in high mortality and rapid dissemination of bacteria. To evaluate septicemia following infection, samples of blood were periodically collected to detect bacteremia. Bacteremia was detected in 9/10 RMs and 7/10 AGMs (Tables 1 and 2). The median times to detection of first bacteremia in animals that became moribund were 56 h (range, 24 to 96 h) and 96 h (range, 32 to 120 h) for the RMs and AGMs, respectively. Bacteremia was detected in only one of the RMs surviving for 45 days postexposure. Out of the 16 RMs and AGMs that had bacteremia, five RMs and four AGMs had bacteremia detected once; four RMs and three AGMs had bacteremia detected on two separate days, with only one RM and one AGM having consecutive days of bacteremia.

In animal models and human melioidosis, rapid bacterial dis-

TABLE 2 Bacteremia in RMs and AGMs following exposure to *B. pseudomallei*

Species	Bacteremia parameter	Prevalence and magnitude of bacteremia on each day postexposure[a]											
		1[b]	2[c]	3	4	5	6	7	14	21	28	35	42
RM	Prevalence (no. with bacteremia/total no.)	4/10	1/10	1/10	2/8	1/4	0/3	0/3	0/3	0/2	0/2	0/2	0/2
	Magnitude (median CFU/ml)	10	10	40	1480	10	NA	NA	NA	NA	NA	NA	NA
AGM	Prevalence (no. with bacteremia/total no.)	1/10	1/10	1/10	5/9	2/4	0/2	0/1	0/1	NA	NA	NA	NA
	Magnitude (median CFU/ml)	20	10	100	20	20	NA	NA	NA	NA	NA	NA	NA

[a] All bacteremia before day 3 was detected when blood was collected every 8 h. NA, not applicable.
[b] Bacteremia was detected at 24 h (two RMs), 32 h (one RM and one AGM), and 40 h (one RM) postexposure.
[c] Bacteremia was detected at 56 h postexposure.

semination is commonly noted following acute infections. To evaluate the bacterial dissemination, samples of lung, liver, spleen, pancreas, and gonads were collected from each animal at necropsy and plated to evaluate positive or negative growth of *B. pseudomallei*. From lung tissue, a total of 9/10 RMs and 10/10 AGMs were culture positive for *B. pseudomallei*. The only RM that was not culture positive was exposed to 1,763 CFU and survived for 45 days. The spleen was also consistently culture positive, with a total of 7/10 RMs and 10/10 AGMs culturing positive. The 3 RMs not culture positive included both RMs that survived for 45 days postexposure. From the liver tissue, a total of 8/10 RMs and 10/10 AGMs were culture positive. The two RMs not culture positive survived for 45 days postexposure. The pancreas was culture positive in 5/10 RMs and 10/10 AGMs. The gonads were culture positive in 7/10 RMs and 6/10 AGMs.

Cytokine and chemokine responses after exposure to *B. pseudomallei*. The magnitudes of the cytokine and chemokine responses were compared between baseline levels and the first 4 days postexposure for interleukin 1β (IL-1β), IL-2, IL-6, IL-8, IL-10, IL-12p70, granulocyte-macrophage colony-stimulating factor (GM-CSF), gamma interferon (IFN-γ), and tumor necrosis factor alpha (TNF-α). In the AGMs, IL-1β (Fig. 4B), IL-6 (Fig. 4D), IL-8 (Fig. 4F), and IFN-γ (Fig. 4H) were observed to increase on day 4 postexposure. In the RMs, IL-1β (Fig. 4A) and IL-6 (Fig. 4C) were the only cytokines observed to significantly increase. It was observed that IL-8 tended to decrease on day 2 postexposure in the RMs (Fig. 4E). IFN-γ showed little overall change in the RMs, but a significant decrease was noted on day 2 postexposure (Fig. 4G). TNF-α generally increased postexposure in both the RMs and AGMs, but the increase was not significant (Fig. 4I and J). No significant changes in IL-2, IL-10, IL-12p70, and GM-CSF were noted in the RMs or AGMs. Differences were noted between the RMs and AGMs for IL-1β ($P < 0.05$), IL-2 ($P < 0.05$), and IFN-γ ($P < 0.05$). In the AGMs, on day 3 and day 4 postexposure, IL-1β was a good predictor of outcome, showing a good correlation between decreased survival time and increased levels (day 3, $P = 0.029$; day 4, $P < 0.001$). Additionally, on day 4 postexposure in the AGMs, IL-6 ($P < 0.001$) and IL-10 ($P = 0.011$) were found to correlate to outcome. No other cytokines were good predictors of outcome, and no cytokines measured in the RMs were predictive of outcome.

Lung pathology. Pulmonary lesions were found to be the most common gross pathology finding in both the RMs and AGMs (Table 3). Abscesses, red mottled noncollapsing lungs, and pleural adhesions were consistent findings (Fig. 5A and B). Foci of necrosis or abscesses were commonly suppurative to caseous nodules, often rimmed by congestion/hemorrhage, beginning to appear in animals that became moribund 3 to 5 days postexposure. The pulmonary lesions ranged from 0.5 to 1.0 cm in diameter in animals that were moribund within 7 days postexposure and from 2.0 to 3.0 cm in two animals on day 14 postexposure. Histologically, necrotic foci affected pulmonary architecture and consisted of extensive necrotic debris admixed with fibrin edema, hemorrhage, numerous degenerate neutrophils, necrotic leukocytes (composed of neutrophils and macrophages), fewer macrophages, lymphocytes, and plasma cells. Lung tissue immediately adjacent to the foci ranged from minimally affected to unaffected (Fig. 5C). Both RMs that survived for 45 days postexposure were noted as having pneumonia, the RM exposed to 6,239 CFU was noted as having a 0.5-cm chronic suppurative abscess on the left inferior lobe, and the RM exposed to 1,763 CFU had pyogranulomatous foci of inflammation in the lungs.

An immunohistopathology assessment was performed to confirm the presence of bacteria within inflammatory sites. A total of six NHPs (three RMs and three AGMs) had lung tissue stained with 3B3-5, a monoclonal mouse antibody for *B. pseudomallei* LPS, and all had positive immunoreactivity. Most of the immunoreactivity was located in the necrotizing foci intracytoplasmically in macrophages and neutrophils, as well as in necrotic debris to include bronchiolar/bronchial exudates (Fig. 5D). Immunoreactivity was minimal in areas with minimal histopathologic lesions.

Ultrastructural analysis of lung was performed to assess intra- or extracellular localization of bacteria. Evaluation of lung tissue from an AGM confirmed the presence of intra- and extracellular bacteria in alveolar macrophages and necrotic debris, respectively. Fibrin was also intermixed with the necrotic debris and extracellular bacteria (Fig. 5E and F).

Lymph node pathology. Lymph node enlargement was the second most common gross finding, often accompanied by congestion (Table 3). The tracheobronchial and mediastinal lymph nodes were the most significantly and consistently enlarged, affecting 6/10 RMs and 7/10 AGMs. Inflammation in the tracheobronchial/mediastinal lymph nodes ranged from minimally neutrophilic to necrotizing foci initially in the subcapsular sinus region to diffuse suppurative inflammation effacing large sections of the lymph nodes. The severity of the affected thoracic lymph nodes was random throughout the study. The inguinal, axillary, and mandibular lymph node inflammation was minimal to mild and predominantly associated with AGMs.

Secondary changes associated with the lymph nodes include

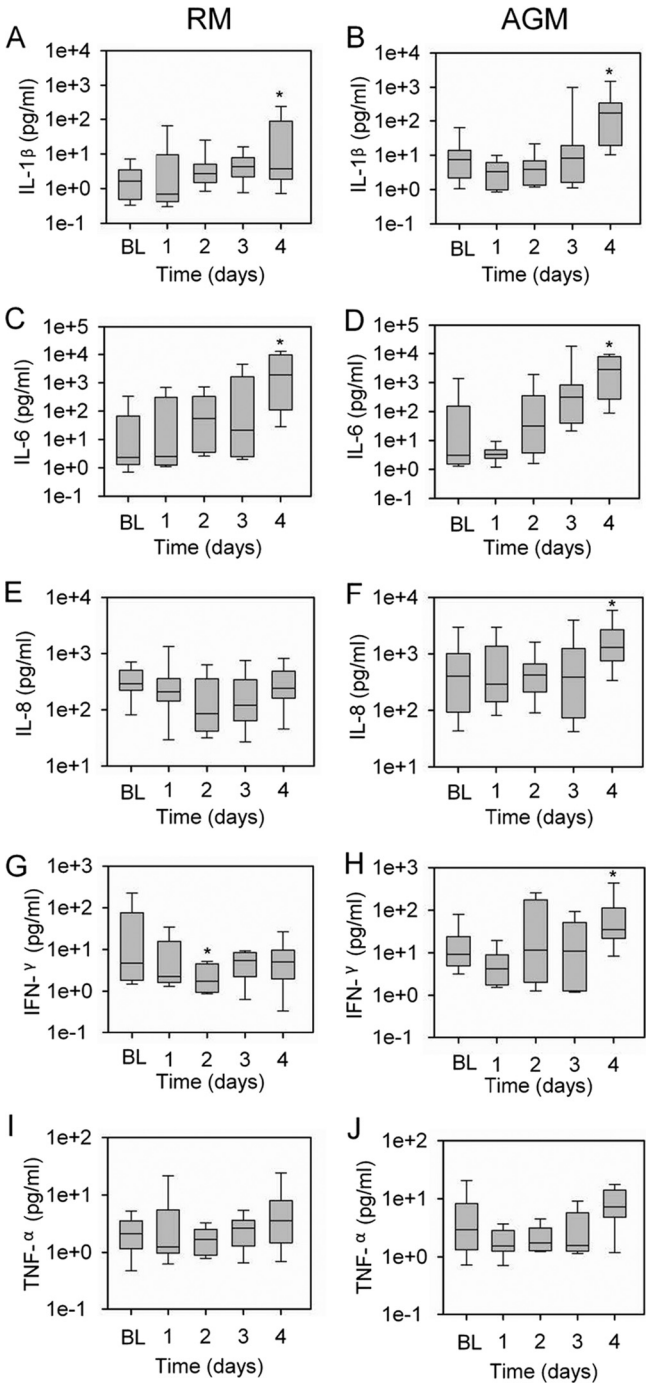

FIG 4 Cytokine and chemokine responses following exposure to *B. pseudomallei*. A significant increase in IL-1β was noted 4 days postexposure for both the RMs (A) and AGMs (B). Similarly, IL-6 had a noticeable increasing trend, with a significant increase above baseline levels (BL) 4 days postexposure in both the RMs (C) and AGMs (D). (E) IL-8 generally did not change for RMs; however, on day 2, there was a noticeable decrease. (F) In the AGMs, IL-8 showed little change until 4 days postexposure, when there was a significant increase. (G and H) IFN-γ was highly variable with little change for RMs, but a significant decrease 2 days postexposure in RMs was noted (G), and a significant increase was noted 4 days postexposure in the AGMs (H). TNF-α was also variable for both the RMs (I) and the AGMs (J), with a general increase for AGMs postexposure. Bars represent the 25th and 75th percentiles (the solid line is the median), and error bars represent the 5th and 95th percentiles. Baseline (BL), day 1, day 2, and day 3, $n = 10$; day 4, $n = 8$ and $n = 9$ for RMs and AGMs, respectively. *, $P < 0.05$.

TABLE 3 Major pathology findings of inhalation melioidosis

Manifestation	Prevalence (no. with manifestation/total no.)	
	RM	AGM
Pneumonia	10/10	10/10
Lymphadenitis	10/10	10/10
Myelitis	6/10	8/10
Splenitis	3/10	6/10
Hepatitis	2/10	4/10
Tonsillitis	2/10	1/10
Nephritis	0/10	1/10
Encephalitis	0/10	1/10
Mild meningeal congestion	5/10	4/10

congestion, histiocytosis, edema, draining hemorrhage, lymphocytic hyperplasia, and lymphocyte depletion. Congestion and histiocytosis were most common but were not associated exclusively with the tracheobronchial/mediastinal lymph nodes. Lymphoid depletion was commonly identified in acute (3 to 6 days postexposure) cases and associated with necrotizing to suppurative tracheobronchial/mediastinal lymph nodes.

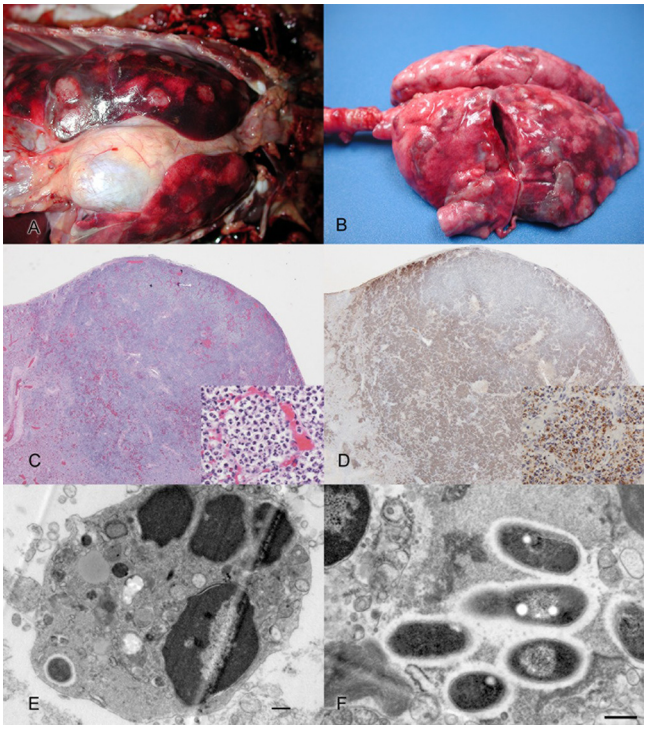

FIG 5 Pulmonary lesions identified 4 days after aerosolization with *B. pseudomallei*. (A and B) The lungs contained several 0.8- to 1.5-cm pale foci that were often elevated from the surface and surrounded by a hyperemic rim of congestion. (C) Low-power magnification (HE; ×4) of pulmonary lesions composed of necrotic debris and inflammatory cells, predominantly degenerate neutrophils (inset, ×40). (D) Immunohistochemistry of the pulmonary lesions, consisting of intracytoplasmic positive immunoreactivity in neutrophils and macrophages and scattered necrotic debris at low power (×4) (inset, ×40). (E) A single bacterium resides within a macrophage in the lung of an AGM. Bar = 500 nm. (F) A small colony of bacteria has been released into the extracellular milieu and is surrounded by necrotic debris and fibrin. Bar = 500 nm.

Lymph nodes rarely had positive immunoreactivity to bacteria; when observed, this was limited to the necrotizing inflammation in the tracheobronchial and mediastinal lymph nodes found in two of the six NHPs reviewed. Corresponding intracytoplasmic positive immunoreactivity occurred rarely in macrophages and neutrophils, predominantly in the subcapsular sinuses.

Ultrastructural examination of the tracheobronchial lymph node from a RM showed large amounts of necrotic debris and fibrin aggregates present within the tissue as well as blood and lymphatic vessels. The structured organization of the lymph node was largely lost; however, bacteria were not observed despite the rare, albeit positive, immunoreactivity.

Spleen and bone marrow pathology. The hematopoietic system consisting of the spleen and bone marrow is known to be involved in melioidosis infections; however, the bone marrow has yet to be extensively evaluated after exposure to *B. pseudomallei*. The spleen and bone marrow were noted as being affected as consistently as the lymph nodes, with the spleen most commonly affected. The spleen was enlarged in 3/10 RMs and 6/10 AGMs (Table 3). Histologically, the splenic lesions consisted of necrotizing inflammation, degenerate neutrophils with low numbers of macrophages, fewer lymphocytes, and plasma cells ranging from small, individual microfoci to larger coalescing lesions. Additionally, four AGMs exhibited mild lymphocytic depletion of the white pulp. The two RMs that survived for 45 days postexposure had a mild splenic lymphocytic hyperplasia. Lesions were more common in AGMs than RMs.

The bone marrow lesions consisted of similar necrotizing inflammation, predominantly of degenerate neutrophils, fewer macrophages, few lymphocytes, and plasma cells (Table 3). This inflammation was found in small and variously sized coalescing foci effacing up to 40% of the reviewed sections, often with normal myeloid and erythroid components adjacent to them. Two AGMs developed concurrent mild myeloid hyperplasia. Additionally, three AGMs exhibited a mild increase in hemosiderosis. Again, lesions were more common in AGMs than RMs. Positive immunoreactivity to bacteria was usually limited to the foci of necrotizing inflammation in both the spleen and the bone marrow. Corresponding intracytoplasmic positive immunoreactivity occurred in low numbers of macrophages and neutrophils in the spleen and bone marrow.

Ultrastructural examination of the spleen from an RM showed a loss of tissue organization, necrotic cells, and sparse intracellular bacteria.

Additional pathology. One AGM had a noteworthy lesion affecting the brain and adrenal gland. The cerebral lesion was a single small focus of perivascular inflammation that was composed of low numbers of lymphocytes, plasma cells, fewer neutrophils, and macrophages (Table 3). The same AGM had a few microfoci of neutrophilic inflammation of adjacent adrenal epithelial cells. There was no identifiable positive immunoreactivity in the adrenal gland. Immunohistochemistry was not used on the cerebral perivascular inflammation. Liver lesions varied greatly among all NHPs. Hepatitis occurred as variably sized foci in 2/10 RMs and 4/10 AGMs (Table 3). Positive immunoreactivity was rarely observed. One AGM had significant lesions in the kidney, although minimal immunoreactivity was noted (Table 3). Tonsillitis was present in 2/10 RMs and one AGM (Table 3). Both RMs with tonsillitis survived for 45 days postexposure. Minimal positive immunoreactivity occurred. Other notable gross abnormalities recorded consisted of mild meningeal congestion, adrenal congestion, hepatomegaly, increased serosanguineous peritoneal fluid, and testicular hemorrhage (Table 3).

DISCUSSION

The objective of this study was to determine if the RM and AGM are appropriate animal models for use as inhalation melioidosis models for evaluation of medical countermeasures. The data presented here indicate that AGMs are highly susceptible to aerosolized *B. pseudomallei* and develop a rapidly lethal pneumonic infection whereas RMs generally develop a lethal infection but can develop subacute pneumonia. Collectively, these data indicate that both RMs and AGMs are reasonable models, with the AGMs being a more appropriate model for medical countermeasure evaluation.

There are limited reports of melioidosis having been studied in an NHP model, with even fewer reports of inhalational melioidosis. One study by Miller et al. (28) challenged RMs by subcutaneous injection and determined that they were relatively resistant to infection (28). It was reported that a localized abscess formed but healed, with no noticeable disease developing. The difference between the study reported here and that performed by Miller et al. (28) is possibly a result of the route of infection, but it is also possibly a result of the strain of *B. pseudomallei*. However, reports of natural outbreaks in NHPs imported from areas of endemicity and recent studies in NHPs by Manzenuik et al. (27) and Nelson et al. (29) support the notion that NHPs are susceptible to infection with *B. pseudomallei* (1, 14, 20, 27, 29). Although historically conflicting data on the susceptibility of NHPs to melioidosis existed, it has become evident with the recent NHP studies and the models presented here that the NHP is a reasonable and valuable model system for studying melioidosis pathogenesis and for medical countermeasure evaluation.

The models described here had consistent disease progression and onset similar to those of acute infection in humans, which is generally described as a quickly progressing disease with onset 1 to 21 days postexposure (3, 8). Both species developed a fulminant pulmonary infection (or bronchopneumonia) and sepsis, with many becoming moribund 3 to 5 days postexposure. This rapid disease onset and progression is typically observed in humans that are suspected of respiratory exposures by aspiration or inhalation (3, 8). Inhalation as a diagnosed route of exposure is difficult to confirm but has been suspected in severe disease in U.S. helicopter crews during the Vietnam War and after extreme-weather events in Northern Australia (7, 8, 17). Aspiration is more easily diagnosed as being the route of exposure and is typically associated with severe melioidosis (4). By a comparison of data from acute human melioidosis cases, many from known aspiration cases, it was evident that the RMs and AGMs develop symptoms resembling those observed in humans. In severe human cases, it is reported that fever presents in 50 to 90% of melioidosis cases, with dyspnea being reported 60 to 80% of the time, accompanied by cough and pneumonia (3, 4, 33). Bacteremia is typically variable but is common in acute melioidosis infections. It is reported that 30 to 90% of cases are positive when admitted to the hospital (8, 25, 33). Similar to what is reported in these cases, the RMs and AGMs presented with fever (100% of the NHPs), dyspnea (85%), pneumonia (100%), neutrophilia (100%), and bacteremia (80%) (Tables 1, 2, and 3).

The characteristic rapid increase in neutrophils is primarily a

result of the high inflammatory response, resulting from an increase in IL-1β, IL-6, IFN-γ, TNF-α, and IL-8 (13, 16). A study by Easton et al. (13) has shown that in C57BL/6 mice, neutrophil recruitment into the lungs reaches a maximum at around day 3 postexposure. In both the RM and AGM models, animals that became moribund 3 to 5 days postexposure showed high numbers of degenerate neutrophils with necrotic debris in the lungs (Fig. 5C and D) and bone marrow. This rapid recruitment to sites of inflammation, such as the lungs, and corresponding destruction of the bone marrow is a likely explanation for the dramatic decrease in neutrophils/leukocytes (Fig. 3) and occasional neutropenia/leukopenia observed in both the RMs and AGMs (Table 1). Similarly, Nelson et al. (29) have recently described a similar occurrence in marmosets.

The increase in proinflammatory cytokines in melioidosis is well documented. Murine models have shown that in BALB/c and C57BL/6 mice, IL-1β, IL-6, IL-10, IFN-γ, and TNF-α are commonly elevated (37, 38). These sets of cytokines have also been seen to be elevated in humans infected with melioidosis (41). This is similar to the observations in the AGMs, in which IL-1β, IL-6, IL-8, IFN-γ, and TNF-α were generally elevated by 4 days postexposure (Fig. 4). Interestingly, the RMs were noted to have a less intense increase in proinflammatory cytokines, much like what has been observed in the C57BL/6 mice, which are generally regarded as more resistant to infection then BALB/c mice (37). Generally, it appears that the AGMs develop a more universal and intense proinflammatory response than the RMs' generally subdued response, a finding which is at least practically in agreement with differences observed between BALB/c and C57BL/6 mice. We also evaluated the relationship between increased cytokine levels and survival time and found that the results in AGMs are in agreement with findings in humans that have indicated that IL-1β is a predictor of poor outcome (41). The levels of IL-1β on day 3 and day 4 in the AGMs were the best predictors of decreased survival time. We also found that on day 4 postexposure, IL-6 and IL-10 were predictive of decreased survival time.

A decrease in circulating platelet levels was observed starting 2 days postexposure (Fig. 3G and H), and ultrastructural analysis of tissues revealed fibrin aggregates in the blood and lymphatic vessels. The excessive aggregation of fibrin in the blood vessels and decrease in circulating platelets indicated intravascular coagulation, which has been associated with high mortality in melioidosis (40). The scope of this study did not explore the coagulation pathways in detail, but previous reports have suggested that in humans and marmosets, the coagulation pathways are significantly altered after exposure to *B. pseudomallei* (29, 42).

The RMs and AGMs all showed extensive and consistent necrotizing inflammation of the lungs, lymphatic system, spleen, and bone marrow (Table 3), with occasional to rare inflammation of the liver, kidney, and brain (Table 3). This pattern of involvement in RMs and AGMs was found to be consistent with reports in human acute melioidosis, which predominantly involves the lungs, lymphatic system, spleen, and liver (32). Less consistently affected are brain, kidney, skin, and skeletal muscle (32). Additionally, the histopathologic findings in the RMs and AGMs support previous findings in NHPs and murine models, which have found that the lungs, lymphatic system, and spleen are commonly affected (19, 23, 27, 29). Overall, the histopathology findings in the RMs and AGMs are in good agreement with those of both human and other NHP models (27, 29, 32). The most noticeable difference in the histopathologic findings between the AGMs and RMs was that AGMs were more consistently noted to have a systemic infection. Although systemic involvement was more frequently noted in AGMs, differences in severity of lesions of the affected areas were not noted between the RMs and AGMs.

The brain was only rarely seen to be involved; however, one AGM had a cerebral lesion and 5/10 RMs and 4/10 AGMs had meningeal congestion (Table 3). Recently, bacteria have been cultured from the brains of AGMs with meningeal congestion (J. J. Yeager, unpublished data). There have been reports of central nervous system (CNS) infections caused by melioidosis, reported primarily in Northern Australia (8, 9). Additionally, CNS involvement has been noted in an RM that was affected by a natural infection (14) Overall, these infections are rare, occurring in less than 10% of all human melioidosis cases (9), but the severity of CNS infections makes them a serious manifestation of melioidosis. There has been a recent study in BALB/c mice that has shown that inhalation of *B. pseudomallei* may result in the bacteria entering the olfactory nerve and entering the brain via that route (30). This has serious implications for natural inhalational exposures or intentional bioterrorist threats. This is a serious manifestation of melioidosis that needs further attention to be fully understood.

Overall, significant clinical or immunological differences between RMs and AGMs were limited. The hematologies of the RMs and AGMs were similar, with no significant difference in neutrophils, lymphocytes, monocytes, or platelets (Fig. 3). Clinical signs and survival postexposure were similar in RMs and AGMs (Table 1 and Fig. 1) except for the two RMs that survived. Histopathologic analysis first indicated that the AGMs were more likely to develop systemic infections than were the RMs. Additional support of this finding comes from the two RMs that survived for 45 days postexposure which were exposed to 6,239 CFU and 1,763 CFU. These two cases reinforced the complexity of melioidosis infections. Both these cases represent two other manifestations of melioidosis: first, a chronic suppurative infection, and second, a latent asymptomatic pyogranulomatous infection. The RM exposed to 1,763 CFU showed minimal clinical or immunological signs of infection after 14 days postexposure; however, histopathologic evaluation found lesions with bacteria within the lungs. The second RM exposed to 6,239 CFU exhibited clear signs of pneumonia at 45 days postexposure, and gross and histopathologic examination indicated an active pneumonic infection with limited systemic involvement. These findings help support the observation that AGMs are more likely to develop acute fulminate pneumonia with systemic involvement whereas RMs may be slightly more resistant to a systemic infection, leading to a more chronic suppurative infection. Although we believe that the RM and the AGM both represent valuable disease models of inhalation melioidosis, the AGM does appear to be the most appropriate model for evaluation of medical countermeasures.

In summary, we investigated the RM and AGM to determine their usefulness as model systems for studying inhalational melioidosis and evaluating medical countermeasures against melioidosis. We set out to determine if both or one of these models closely resembles the disease reported in acute human melioidosis. The data presented here support that RMs and AGMs develop a disease that resembles acute human melioidosis and that both represent a valuable model for studying the pathogenesis of *B. pseudomallei*. However, for the purpose of evaluating therapeutic

treatments and future vaccines, the AGM does appear to be a more valuable and appropriate model system.

ACKNOWLEDGMENTS

We thank Dave Waag for supplying the strain of *B. pseudomallei* and the monoclonal antibody used in these experiments. We also thank Tony Alves, Dave DeShazer, and Dave Waag for critically reviewing the manuscript. We thank Sarah Norris for her assistance with statistical analysis. We also thank all the support staff involved in the study from the Center for Aerobiological Sciences, Veterinary Medicine Division and Pathology Division.

This project was supported by the Defense Threat Reduction Agency—Transformational Medical Technology Initiative, plan number 108574.

Opinions, interpretations, conclusions, and recommendations are those of the authors and are not necessarily endorsed by the U.S. Army.

REFERENCES

1. **Butler TM, Schmidt RE, Wiley GL.** 1971. Melioidosis in a chimpanzee. Am. J. Vet. Res. **32**:1109–1117.
2. **Cheng AC.** 2010. Melioidosis: advances in diagnosis and treatment. Curr. Opin. Infect. Dis. **23**:554–559.
3. **Cheng AC, Currie BJ.** 2005. Melioidosis: epidemiology, pathophysiology, and management. Clin. Microbiol. Rev. **18**:383–426.
4. **Chierakul W, et al.** 2005. Melioidosis in 6 tsunami survivors in Southern Thailand. Clin. Infect. Dis. **42**:982–990.
5. **Chin C-Y, Monack DM, Nathan S.** 2010. Genome-wide transcriptome profiling of a murine acute melioidosis model reveals new insights into how *Burkholderia pseudomallei* overcomes host innate immunity. BMC Genomics **11**:672.
6. **Currie BJ, Fisher DA, Howard DM, Burrow JNC.** 2000. Neurological melioidosis. Acta Trop. **74**:145–151.
7. **Currie BJ, Dance DAB, Cheng AC.** 2008. The global distribution of *Burkholderia pseudomallei* and melioidosis: an update. Trans. R. Soc. Trop. Med. Hyg. **102**(Suppl 1):S1–S4.
8. **Currie BJ, Jacups SP.** 2003. Intensity of rainfall and severity of melioidosis, Australia. Emerg. Infect. Dis. **9**:1538–1542.
9. **Currie BJ, Ward L, Cheng AC.** 2010. The epidemiology and clinical spectrum of melioidosis: 540 cases from the 20 year Darwin prospective study. PLoS Negl. Trop. Dis. **4**:e900. doi:10.1371/journal.pntd.0000900.
10. **Dabisch PA, Kline J, Lewis C, Yeager J, Pitt MLM.** 2010. Characterization of a head-only aerosol exposure system for nonhuman primates. Inhal. Toxicol. **22**:224–233.
11. **Dance DAB.** 1991. Melioidosis: the tip of the iceberg? Clin. Microbiol. Rev. **4**:52–60.
12. **DeShazer D, Brett PJ, Carlyon R, Woods DE.** 1997. Mutagenesis of *Burkholderia pseudomallei* with Tn5-OT182: isolation of motility mutants and molecular characterization of the flagellin structural gene. J. Bacteriol. **179**:2116–2125.
13. **Easton A, Haque A, Chu K, Lukaszewski RA, Bancroft GJ.** 2007. A critical role for neutrophils in resistance to experimental infection with *Burkholderia pseudomallei*. J. Infect. Dis. **195**:99–107.
14. **Fritz PE, Miller JG, Slayter M, Smith TJ.** 1986. Naturally occurring melioidosis in a colonized rhesus monkey (*Macaca mulatta*). Lab. Anim. **20**:281–285.
15. **Hartings JM, Roy CJ.** 2004. The automated bioaerosol exposure system: preclinical platform development and a respiratory dosimetry application with nonhuman primates. J. Pharmacol. Toxicol. Methods **49**:39–55.
16. **Hii C-S, et al.** 2008. Interleukin-8 induction by *Burkholderia pseudomallei* can occur without Toll-like receptor signaling but requires a functional type III secretion system. J. Infect. Dis. **197**:1537–1547.
17. **Howe C, Sampath A, Spotniz M.** 1971. The *Pseudomallei* group: a review. J. Infect. Dis. **124**:598–606.
18. **Inglis TJJ, Rolim DB, Sousa ADQ.** 2006. Melioidosis in the Americas. Am. J. Trop. Med. Hyg. **75**:947–954.
19. **Jeddeloh JA, Fritz DL, Waag DM, Hartings JM, Andrews GP.** 2003. Biodefense-driven murine model of pneumonic melioidosis. Infect. Immun. **71**:584–587.
20. **Kaufmann AD, et al.** 1970. Melioidosis in imported primates nonhuman. J. Wildl. Dis. **6**:211–219.
21. **Laws TR, Smither SJ, Lukaszewski RA, Atkins HS.** 2011. Neutrophils are the predominant cell-type to associate with *Burkholderia pseudomallei* in a BALB/c mouse model of respiratory melioidosis. Microb. Pathog. **51**:471–475.
22. **Lazar Adler NR, et al.** 2009. The molecular and cellular basis of pathogenesis in melioidosis: how does *Burkholderia pseudomallei* cause disease? FEMS Microbiol. Rev. **33**:1079–1099.
23. **Lever MS, Nelson M, Stagg AJ, Beedham RJ, Simpson AJH.** 2009. Experimental acute respiratory *Burkholderia pseudomallei* infection in BALB/c mice. Int. J. Exp. Pathol. **90**:16–25.
24. **Limmathurotsakul D, et al.** 2010. Increasing incidence of human melioidosis in Northeast Thailand. Am. J. Trop. Med. Hyg. **82**:1113–1117.
25. **Limmathurotsakul D, et al.** 2011. Repeat blood culture positive for *B. pseudomallei* indicates an increased risk of death from melioidosis. Am. J. Trop. Med. Hyg. **84**:858–861.
26. **Loveleena Chaudhry R, Dhawan B.** 2004. Melioidosis; the remarkable imitator: recent perspectives. J. Assoc. Physicians India **52**:417–420.
27. **Manzenuik IN, et al.** 1999. *Burkholderia mallei* and *Burkholderia pseudomallei*. Study of immuno- and pathogenesis of malleus and melloidosis. Antibiot. Khimioter. **4**:21–26.
28. **Miller WR, Pannell L, Cravitz L, Tanner WA, Rosebury T.** 1948. Studies on certain biological characteristics of *Maleomyces mallei* and *Malleomyces pseuduomallei* II. Virulence and infectivity for animals. J. Bacteriol. **55**:127–135.

28a. **National Research Council.** 2011. Guide for the care and use of laboratory animals, 8th ed. National Academies Press, Washington, DC.

29. **Nelson M, et al.** 2011. Development of an acute model of inhalational melioidosis in the common marmoset (*Callithrix jacchus*). Int. J. Exp. Pathol. **92**:428–435.
30. **Owen SJ, et al.** 2009. Nasal-associated lymphoid tissue and olfactory epithelium as portals of entry for *Burkholderia pseudomallei* in murine melioidosis. J. Infect. Dis. **199**:1761–1770.
31. **Parameswaran U, Baird R, Ward L, Currie BJ.** 2012. Melioidosis at Royal Darwin Hospital in the big 2009-2010 wet season: comparison with the preceding 20 years. Med. J. Aust. **10**:345–348.
32. **Piggott J, Hochholzer L.** 1970. Human melioidosis: a histopathologic study of acute and chronic melioidosis. Arch. Pathol. **90**:101–111.
33. **Rammaert B, et al.** 2011. Pulmonary melioidosis in Cambodia: a prospective study. BMC Infect. Dis. **11**:126.
34. **Saravu K, et al.** 2008. Melioidosis—a case series from south India. Trans. R. Soc. Trop. Med. Hyg. **102**:S18–S20.
35. **Tan G-YG, et al.** 2008. *Burkholderia pseudomallei* aerosol infection results in differential inflammatory responses in BALB/c and C57Bl/6 mice. J Med. Microbiol. **57**:508–515.
36. **Treviño SR, et al.** 2006. Monoclonal antibodies passively protect BALB/c mice against *Burkholderia mallei* aerosol challenge. Infect. Immun. **74**:1958–1961.
37. **Ulett GC, Ketheesan N, Hirst RG.** 2000. Cytokine gene expression in innately susceptible BALB/c mice and relatively resistant C57BL/6 mice during infection with virulent *Burkholderia pseudomallei*. Infect. Immun. **68**:2034–2042.
38. **Warawa JM.** 2010. Evaluation of surrogate animal models of melioidosis. Front. Microbiol. **1**:141.
39. **White NJ.** 2003. Melioidosis. Lancet **361**:1715–1722.
40. **Wiersinga WJ, et al.** 2008. Activation of coagulation with concurrent impairment of anticoagulant mechanisms correlates with a poor outcome in severe melioidosis. J. Thromb. Haemost. **6**:32–39.
41. **Wiersinga WJ, et al.** 2007. High-throughput mRNA profiling characterizes the expression of inflammatory molecules in sepsis caused by *Burkholderia pseudomallei*. Infect. Immun. **75**:3074–3079.
42. **Wiersinga WJ, van der Poll T.** 2009. Immunity to *Burkholderia pseudomallei*. Curr. Opin. Infect. Dis. **22**:102–108.